Exact Modelling of the Phases at the Triple Point of Zirconia

Kai Hormann
Department of Informatics
Clausthal University of Technology

Johannes Zimmer
Department of Mathematical Sciences
University of Bath

Abstract

We propose a general method for modelling transformation paths of multi-phase materials such that elastic moduli can be fitted exactly. The energy landscape obtained in this way is global and automatically enjoys the correct symmetries. The method is applied to the triple point of zirconia, where tetragonal, orthorhombic (orthoI), and monoclinic phases meet. An explicit and relatively simple expression yields a phenomenological model in the two-dimensional space spanned by a set of order parameters. We also show how to extend this energy to the apparently first fully three-dimensional model with an exact fit of all given elastic moduli.

1 Introduction

We propose a method to derive an explicit phenomenological model of several coexisting stable phases and the relevant transformation paths. The focus is on solid-solid phase transitions. A detailed understanding of the transformation mechanisms is essential both for theory and applications of phase transitions. In theory, the framework of the analysis of solid-solid phase transformations is well established: since diffusion and re-ordering processes are usually negligible, these materials can be well approximated in the realm of nonlinear elasticity. In practice, any constitutive modelling requires an explicit expression for the energy density. It is remarkable that there are very few explicit energy densities available for three space dimensions that interpolate key data such as elastic moduli exactly.

The relative shortage of explicit expressions for energy functions is even more surprising in light of the subject's long history. The analysis of strain- and temperature-dependent energy functions was initiated by Landau [15]. A more recent line of investigation based on the Cauchy-Born hypothesis in continuum mechanics can be traced back to Ericksen [5]. A common method for deriving energy densities is to expand the energy function in invariant polynomials of lowest order and fit as many degrees of freedom as possible, or to obtain a best fit in some error norm. As for the triple point of zirconia (ZrO_2), when working with an expansion in invariant polynomials, it requires considerable ingenuity to obtain a reasonable or good match of most moduli [6]; not all moduli can be fitted this way, let alone further information of the transformation path. This observation is not surprising given that polynomials offer little flexibility to control the energy along (transformation) paths. Is has been pointed out [9] that the minimal set of order parameters may lead to unrealistically high estimates for the thermal activation energy. Consequently, to determine the energy barrier correctly, non-symmetry-breaking order parameters or, more specifically, invariant polynomials of higher order are employed in [9]. With the advent of *ab initio* calculations, data for the transformation point becomes available, and it is thus reasonable to ask for a method that can provide an exact reproduction of experimental data obtained along the entire transformation path, including data at the stable phases. For theory and applications of solid phase transitions alike, it is of general interest to have a methodology which allows to fit experimental data for multi-phase materials in a simple and phenomenological, yet natural way.

To achieve this aim, we propose an intuitive method. The stable phases are first connected by a *path* that mimics the kinematic transformation path (if measurements are available). The path is modelled in the space of invariant polynomials so that the correct symmetries are automatically ensured. In Fig. 1 (left) such a path is visualized for a material with three stable phases. The wells in the figure

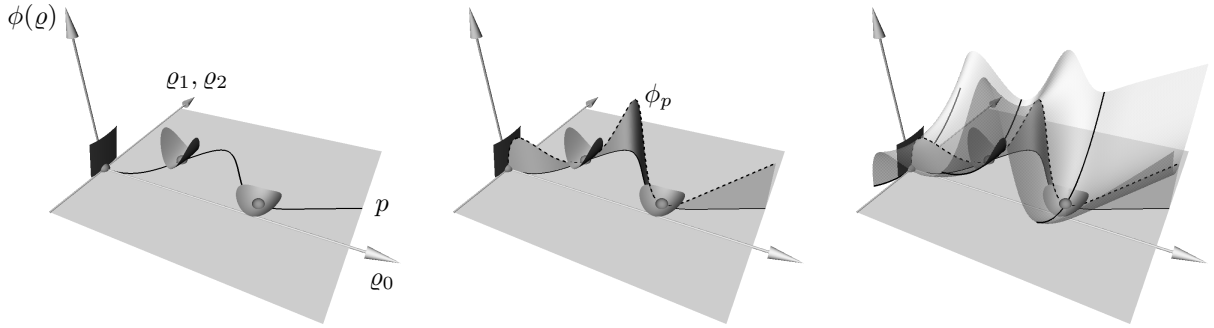

Figure 1: Left: Visualization of the input data in a space of invariant polynomials of the strain tensor; see Section 2.3. Here, the space of invariant polynomials is visualized as a plane. The stable phases are marked by spheres and the moduli are indicated by quadratic wells around the phases. A transformation *path* p connecting the stable phases is indicated as a solid line. It is defined in the space of invariant polynomials and parameterized by the order parameter ϱ_0. Middle: A *profile* ϕ_p (dashed) is defined along the path. Right: The growth away from the path is modelled by a family of *paraboloids*, parameterized by the path so that the given elastic moduli are interpolated.

indicate the respective elastic moduli and $\varrho_0, \varrho_1, \varrho_2$ are the symmetry-adapted coordinates we employ to deal with the crystalline symmetry (see Section 2.3 below for details). The path is parameterized by a suitable invariant, here ϱ_0. We remark that in general the symmetry-adapted coordinates may form a collection of manifolds. The framework presented here allows under weak assumptions a reduction of this nonlinear setting to a linear one, without loss of generality. Consequently, the coordinates are visualized as a plane in Fig. 1. A *profile* then models the energy along the path and thus has minima at the stable phases and energy barriers in between; see Fig. 1 (middle). In addition, we model the growth of the energy away from the path. Here, a quadratic growth is chosen, which is sufficient and keeps the global order low. We first construct at each stable phase a *paraboloid* that interpolates the elastic moduli locally, and then interpolate between them along the path. This interpolation can be interpreted as a continuously deforming paraboloid that slides along the profile curve and blends one locally fitted paraboloid into the next; see Fig. 1 (right). A plot of a schematic energy landscape obtained this way is shown in Fig. 2. In Section 3 we explain why this *ansatz* gives enough freedom to fit all elastic moduli exactly.

To demonstrate that this approach is capable of fitting available data, we consider zirconia as a case study. This choice is motivated by Gibb's phase rule, according to which a one-component system can have at most three phases in coexistence, namely at the triple point, which occurs at one specific combination of pressure and temperature. Thus, a triple point is the most complicated scenario for single-component materials. Zirconia has a triple point with tetragonal, orthorhombic (orthoI) and monoclinic phases in coexistence. While the analysis of phase transformations in zirconia is of interest for applications such as toughening of ceramics, the high pressure and temperature at the triple point render experimental investigations difficult. Numerical simulations offer an alternative, but are currently hampered by a lack of a simple energy function that has minimizers only at experimentally observed phases and fits available experimental data exactly. We give such an expression in Section 3.3.

For the triple point of zirconia, a simple count of the degrees of freedoms shows that an invariant polynomial of lowest order does not offer enough parameters to match all moduli. Higher-order invariant polynomials provide a theoretical remedy for this problem, but are rarely used in practice. One problem is that the calculations for the derivation become very cumbersome, and it can be hard to verify that higher-order polynomials do not introduce spurious minima. In addition, the steep growth of higher-order polynomials often poses a challenge for simulations. At present, the generic Landau strain-energy function constructed by Truskinovsky and Zanzotto [19] and its augmentation by four new coupling terms to fit experimental data [6] seem to be the best three-dimensional energies for zirconia available. In two space dimensions, an approach using splines is able to match all available moduli exactly [4].

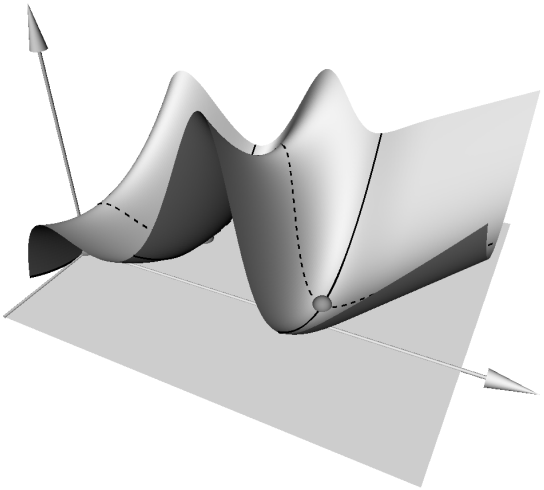

Figure 2: A schematic plot of the final energy landscape.

While the path from the tetragonal phase to an orthorhombic minimum for a polynomial energy of lowest order is extremely shallow, splines offer enough flexibility to model a significant energy barrier. Straightforward numerical simulations with a spline energy can capture the corresponding pattern formation, while they fail to do so for a polynomial energy [4]. However, the spline energy in [4] itself involves a finite element simulation and cannot be written down in a simple and concise form; it is also not immediate how to extend it to three dimensions.

The energy in [4] is continuously differentiable (C^1) and the authors report that no spurious effects stemming from the discontinuity in the elastic moduli were ever observed in numerical studies of boundary value problems. This is in line with other simulations with piecewise defined C^1 energy densities [12]. However, we derive here an energy that is twice continuously differentiable (C^2) since the relevant data involves derivatives up to the second order. Moreover, the construction could easily be extended to fit an energy density with an arbitrary degree of smoothness.

The framework proposed in this paper renders the task of fitting parameters remarkably simple, which could signify that the construction has a deeper physical significance. Specifically, for a transition characterized by the softening of a modulus (like the tetragonal-orthorhombic transition considered here) the chosen path seems to capture the softening remarkably well. Polynomials, on the other hand, are in general too rigid to accurately model a path determined by a softening direction. Further, a polynomial expansion of the energy for CuAlNi [8] does not match all elastic moduli, while an approach similar to the one advocated here does provide a perfect fit for InTl [11], which, like CuZnAl, can undergo a cubic-to-monoclinic transition. In general, non-polynomial energy densities have been found to be a good approximation for InTl [13].

2 Relevant Data for Zirconia

2.1 Transformation paths in zirconia

Zirconia has a triple point near 1.8 GPa and 840 K, where a tetragonal (t), an orthorhombic (o) and a monoclinic (m) phase meet. A quick review of the crystallographic aspects of these phases is included here for the reader's convenience. We choose the tetragonal phase as reference configuration; see Fig. 3 for the relevant primitive tetragonal Bravais lattice. The lattice is spanned by three mutually orthogonal basis vectors c_1, c_2 and c_3. It is easy to verify that $R^{\pi}_{c_1}$ and $R^{\pi/2}_{c_3}$ generate the tetragonal point group T_3, where R^{α}_{c} denotes the rotation with angle α about axis c (only orientation-preserving symmetry operations are considered in this paper). We restrict the crystallographic discussion to skeletal lattices; a visualization of the movements of the atoms inside the skeletal lattices is given in [6].

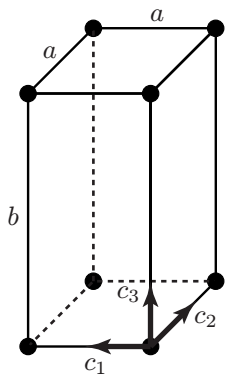

Figure 3: Tetragonal phase with lattice parameters a and b; c_1, c_2 and c_3 denote the axes.

There are two orthorhombic and five monoclinic subgroups and it can be seen that there are four essentially different t–o–m paths [19], going from the tetragonal phase through an orthorhombic to a monoclinic phase. Based on the best-established t–o orientational relationship of the respective axes and the coordination of O atoms with the Zr atoms, a transition path has been suggested [19] which involves the monoclinic group $M_3 := \{1, R^\pi_{c_3}\}$ generated by $R^\pi_{c_3}$ and the orthorhombic group $O_{123} := \{1, R^\pi_{c_1}, R^\pi_{c_2}, R^\pi_{c_3}\}$. Though alternative kinematic paths for the phase transformations in zirconia have been suggested (e.g., [1, 17]), we follow [19] in considering the transformation mechanism

$$T_3 \to O_{123} \to M_3.$$

It is known that the bifurcation associated with the transition $T_3 \to O_{123}$ originates from the softening of the tetragonal modulus $C_{11} - C_{12}$, while the path $T_3 \to M_3$ does not directly correspond to a softening of a tetragonal modulus [6]. This seems natural in light of the separation of the tetragonal and the monoclinic phases by the orthorhombic phase, which makes the $T_3 \to M_3$ transition appear as consecutive bifurcation.

The cubic, tetragonal and monoclinic phases of ZrO_2 have been investigated with lattice dynamics in [14], where the phonon vibrations and the density of states for those phases were determined with the VASP code for ground state calculations combined with the direct method for dynamics.

2.2 Coordinates of the stable phases

Let $y(x)$ denote the deformation at a point x. The free-energy density per unit reference volume, henceforth energy function for short, is a function of the deformation gradient $F_{jk} := \frac{\partial y_j}{\partial x_k}$. By frame indifference, the energy function Φ can be written as a function of $C := F^T F$ or equivalently in terms of the Green-St. Venant strain tensor $E := \frac{1}{2}(F^T F - \mathrm{Id})$. In Voigt's notation,

$$E = \begin{pmatrix} e_1 & \frac{1}{2}e_6 & \frac{1}{2}e_5 \\ \frac{1}{2}e_6 & e_2 & \frac{1}{2}e_4 \\ \frac{1}{2}e_5 & \frac{1}{2}e_4 & e_3 \end{pmatrix}$$

with $e_j \in \mathbb{R}$, $j = 1, \ldots, 6$. The energy $\Phi = \Phi(e_1, \ldots, e_6)$ has to be invariant under the tetragonal point group T_3.

We calculate the position of the t–o–m phases in strain space for 1.8 GPa and 840 K from data for the relevant lattice parameters in [6]. The location of the t-o-m phases in strain space is listed in Table 1.

	tetragonal	orthorhombic	monoclinic
e_1	0.0	$9.39046 \cdot 10^{-3}$	$4.68924 \cdot 10^{-2}$
e_2	0.0	$-5.39105 \cdot 10^{-3}$	$8.50962 \cdot 10^{-3}$
e_3	0.0	$1.71769 \cdot 10^{-2}$	$-5.33516 \cdot 10^{-4}$
e_4	0.0	0.0	0.0
e_5	0.0	0.0	0.0
e_6	0.0	0.0	$-3.28543 \cdot 10^{-1}$

Table 1: The minima in strain space, calculated for 1.8 GPa and 840 K from data for the relevant lattice parameters in the Appendix of [6]. The data is rounded to the 5th digit.

2.3 Symmetry constraints

For the t-o-m transition under consideration, a set of order parameters is given by $e_1 - e_2$ and e_6. Since the transition at the triple point can be described in terms of the order parameters only, we first derive an energy in e_1, e_2 and e_6 and later augment this energy to an energy that depends on the full strain tensor. Both for the reduced and the full set of strain variables, we first identify a suitable basis (a Hilbert basis, see Section 2.3.1) of polynomials $\varrho := (\varrho_0, \dots, \varrho_{n-1})$, where each polynomial depends on the strain variables. We then construct the energy as a function $\phi(\varrho)$, and finally the energy in strain space for $e := (e_1, \dots, e_6)$ is $\Phi(e) := \phi(\varrho(e))$.

2.3.1 Invariants for the Landau contribution

The first step in the construction is to incorporate the symmetry constraints of the tetragonal point group. As the order parameters show, the t–o–m symmetry breaking takes place in the c_1-c_2-plane shown in Fig. 3. Thus, we restrict our attention to the corresponding two-dimensional subspace spanned by c_1 and c_2; the strain space is then spanned by the three strain variables e_1, e_2 and e_6. For this subspace, the three polynomials

$$\begin{aligned} \varrho_0(e_1, e_2, e_6) &:= (e_1 - e_2)^2, \\ \varrho_1(e_1, e_2, e_6) &:= e_1 + e_2, \\ \varrho_2(e_1, e_2, e_6) &:= e_6^2 \end{aligned} \tag{1}$$

are invariant under the (restriction of the) tetragonal point group. In addition, these polynomials have the special property that every polynomial $\tilde{\varrho}$ with this invariance can be written as $\tilde{\varrho}(e_1, e_2, e_6) = P(\varrho_0, \varrho_1, \varrho_2)$ for some polynomial P. The mathematical background for this statement is given in [21, 4]. In a nutshell, by Hilbert's Theorem [20], there is a basis $\varrho_0, \dots, \varrho_{n-1}$ such that every invariant polynomial can be written as a polynomial of the polynomial basis, and by Chevalley's Theorem [3, Theorem A], there has to be a basis with $n = 3$ elements for the tetragonal point group. Since the polynomials in (1) are of lowest degree, they form such a basis. For us, it is convenient to introduce invariants in the order parameters $e_1 - e_2$ and e_6, which is why the basis chosen here differs from the one of [4].

We observe that any function of the polynomials in (1) automatically enjoys the correct symmetry: points in strain space that are mapped to each other under tetragonal symmetry are mapped by $\varrho := (\varrho_0, \varrho_1, \varrho_2)$ to the same point, while points that are not symmetry related are mapped to different points by ϱ. The image of the strain space $\mathbb{R}^3$ under the map ϱ is called *orbit space*. Any function defined in orbit space automatically exhibits the correct symmetries. Here, the orbit space for the Landau contribution is the quadrant

$$\{(\varrho_0, \varrho_1, \varrho_2) \mid \varrho_0 \geq 0 \text{ and } \varrho_2 \geq 0\} \tag{2}$$

and the position of the stable phases in orbit space is recorded in Table 2.

	tetragonal	orthorhombic	monoclinic
ϱ_0	0.0	$2.18493 \cdot 10^{-4}$	$1.47324 \cdot 10^{-3}$
ϱ_1	0.0	$3.99941 \cdot 10^{-3}$	$5.54020 \cdot 10^{-2}$
ϱ_2	0.0	0.0	$1.07941 \cdot 10^{-1}$
ϱ_3	0.0	$1.71769 \cdot 10^{-2}$	$-5.33516 \cdot 10^{-4}$

Table 2: The location of the minima in orbit space, calculated for the strain data given in Table 1. The polynomials $\varrho_4, \dots, \varrho_7$ in (3) as well as ϱ_8, ϱ_9 in (5) vanish at all three phases. The data is rounded to the 5th digit.

2.3.2 Invariants in the three-dimensional setting

Analogously to the two-dimensional basis in (1), the eight invariant polynomials

$$\begin{aligned}
\varrho_0(e_1, \dots, e_6) &:= (e_1 - e_2)^2, \\
\varrho_1(e_1, \dots, e_6) &:= e_1 + e_2, \\
\varrho_2(e_1, \dots, e_6) &:= e_6^2, \\
\varrho_3(e_1, \dots, e_6) &:= e_3, \\
\varrho_4(e_1, \dots, e_6) &:= e_4^2 + e_5^2, \\
\varrho_5(e_1, \dots, e_6) &:= e_4^2 e_5^2, \\
\varrho_6(e_1, \dots, e_6) &:= e_4 e_5 e_6, \\
\varrho_7(e_1, \dots, e_6) &:= e_1 e_4^2 + e_2 e_5^2.
\end{aligned} \tag{3}$$

form a basis in the three-dimensional setting for the full strain tensor with strain variables $e_1, \dots, e_6$.

We computed these invariants with the library finvar.lib of Singular [10]. However, tetragonal invariants can also be read off from the literature [18]. In the three-dimensional setting, we employ the same notation and terminology as introduced for the Landau framework in Section 2.3.1.

We remark that it is also possible to work in symmetry-adapted coordinates, e.g., $y_1 := e_1+e_2+e_3$ to characterize homogeneous dilations, $y_2 := \frac{1}{6}(e_1 + e_2 - 2e_3)$, $y_3 := \frac{1}{\sqrt{2}}(e_1 - e_2)$, $y_j := e_j$ for $j \in \{4, 5, 6\}$. This has been done successfully in [6] to simplify the calculations. Yet, in the framework presented here, it is not less convenient to work directly in strain coordinates.

3 The Path-Profile Construction

3.1 Concept

The proposed construction relies on three simple ingredients: a *path* in the orbit space to model the kinematic transformation path, a *profile* to model the energy along the path, and a *paraboloid* to model the growth away from the path.

The invariance of the energy will be automatically obtained by deriving the energy in the space of invariants, that is, the image of the strain space under the mapping $\varrho := (\varrho_0, \dots, \varrho_{n-1})$; in the two-dimensional Landau setting, we have $n = 3$ (see Section 2.3.1), while $n = 8$ in the full three-dimensional setting (see Section 2.3.2).

The *path* must interpolate all stable phases. Here, we select one order parameter to parameterize the path. Specifically, we work with ϱ_0, though other choices are possible as well. Since ϱ_0 is an order parameter, its evaluations at the tetragonal, orthorhombic and monoclinic phases are mutually different. The ordering is such that the orthorhombic phase separates the tetragonal phase on the left from the monoclinic phase on the right. We then construct a mapping $\pi\colon \mathbb{R} \to \mathbb{R}^{n-1}$ that interpolates the three phases located at $\varrho^\star = (\varrho_0^\star, \dots, \varrho_{n-1}^\star)$ for $\star \in \{\mathrm{t}, \mathrm{o}, \mathrm{m}\}$ in the sense that $\pi(\varrho_0^\star) = (\varrho_1^\star, \dots, \varrho_{n-1}^\star)$. Note that the $n-1$ components π_j of π can be modelled independently of each other. The path p can then

be seen either as the graph of the function π, that is, $p := \{(\varrho_0, \pi(\varrho_0)) \mid \varrho_0 \in \mathbb{R}\} \subset \mathbb{R}^n$, or as the zero-set of the mapping

$$\psi\colon \mathbb{R}^n \to \mathbb{R}^{n-1}, \qquad \varrho \mapsto (\varrho_i - \pi_i(\varrho_0))_{i=1,\dots,n-1},$$

$p = \{\varrho \in \mathbb{R}^n \mid \psi(\varrho) = (0,\dots,0)\}$. It is then clear that the three phases lie on the path: $\varrho^{\mathrm{t}}, \varrho^{\mathrm{o}}, \varrho^{\mathrm{m}} \in p$. This path approximates the kinematic transition path and it would not be difficult to accommodate any explicit knowledge of the transformation path, such as the position of saddle points of the energy. For zirconia, no exact data seems to be available for the kinematic transformation path other than the position of the stable phases; we thus choose a path that simply interpolates between the stable phases. Some care must be taken that the path remains within the orbit space $\varrho(\mathbb{R}^3)$ for the Landau part, respectively $\varrho(\mathbb{R}^6)$ in the three-dimensional setting. This is since the orbit space is defined by homogeneous polynomials, which results in a half-space if the degree is even. For example, the orbit space (2) for the Landau contribution in Section 2.3.1 is only a quadrant of $\mathbb{R}^3$ because ϱ_0 and ϱ_2 are polynomials of even degree.

The *profile* must have global minima at the stable phases, and without loss of generality, we can choose zero as value there. We remark that the method proposed here is also suited for fitting wells of unequal height, for example for a loading experiment. Let ϕ_p denote the energy along the path; obviously, ϕ_p has to be non-negative, $\phi_p\colon \mathbb{R} \to \mathbb{R}_0^+$. This profile models the energy barriers (that is, saddles in the three-dimensional energy landscape) and the wells along the path p. Fig. 1 (middle) shows such a profile construction.

Finally, a *paraboloid* is employed to model the growth of the energy away from the transition path. This choice mirrors the ansatz with invariant polynomials of lowest order. Using quadratic functions for this purpose results in the slowest possible growth of the energy for which the moduli can be fitted, and simultaneously yields the lowest degree functions of the invariants. In order to fit the moduli of elastic phases at the boundary of the orbit space, we need to further introduce a linear contribution in the invariant polynomials of even degree (cf. the linear behaviour in ϱ_0 for the stable phase at the boundary in Fig. 1). Together with a properly chosen path and profile, the combination of linear and quadratic contributions allows us to match all prescribed elastic moduli at given phases exactly. The paraboloid can be thought of as a lowest order ansatz to match elastic moduli at one phase, and then modify it continuously along the path so as to match the moduli at the other phases as well. This is similar in spirit to a lowest order polynomial ansatz, where often a paraboloid is introduced to fit the moduli at the parent phase, and then additional invariants are introduced to match moduli at the other phases as good as possible. This *sliding* paraboloid gives us the freedom to achieve the same goal in a simple fashion without having to compromise in the quality of the approximation at some phases. In the examples discussed below, it is immediate to verify that the interpolated paraboloid remains positive definite, while the linear contributions for quadratic invariants are always non-negative. We denote the paraboloid by $H\colon \mathbb{R} \to \mathbb{R}^{(n-1)\times(n-1)}$ with $H = (h_{jk})_{j,k=1,\dots n-1}$ and remark that it suffices to choose H symmetric, $h_{jk} = h_{kj}$. The linear contribution is denoted $\eta\colon \mathbb{R}^n \to \mathbb{R}_0^+$.

The *energy* is then of very simple form, namely

$$\phi(\varrho) := \phi_p(\varrho_0) + \psi(\varrho)^T H(\varrho_0)\psi(\varrho) + \eta(\varrho). \tag{4}$$

We show below that this ansatz gives enough freedom to match the available data for zirconia. The path, the profile and the paraboloid enter as parameters into the fitting process at the phases.

The specific choice of the terms in (4) will be influenced by the requirement that the only global minima of ϕ are at the given phases. Specifically, we ensure that the energy $\widehat{\phi}(\varrho) := \phi_p(\varrho_0)+\psi(\varrho)^T H(\varrho_0)\psi(\varrho)$ without the linear term has no other global minima, which is guaranteed by two observations. On the one hand, we take care that the paraboloid $H(\varrho_0)$ is always positive definite so that $\widehat{\phi}(\varrho)$ is locally decreasing in at least one direction at any $\varrho \notin p$. On the other hand, the path p itself is constructed in such a way that it only has the three prescribed minima. The linear term $\eta(\varrho)$ is constructed such that it is non-negative everywhere and vanishes at the three phases. We remark that the linear term deforms the path of lowest energy. Consequently, the path p alone does not determine the physical transition path and the correction by the linear term has to be taken into account.

Modulus	tetragonal	orthorhombic	monoclinic
C_{11}	340.0	300.0	312.0
C_{12}	33.0	33.0	35.2
C_{13}	160.0	$\star$	155.0
C_{16}			3.2
C_{22}	$= C_{11}$	350.0	350.0
C_{23}	$= C_{13}$	$\star$	171.0
C_{26}			4.3
C_{33}	325.0	$\star$	341.0
C_{36}			9.4
C_{44}	66.0	$\star$	101.0
C_{45}			-13.9
C_{55}	$= C_{44}$	$\star$	81.6
C_{66}	95.0	90.0	66.3

Table 3: Elastic constants of the tetragonal and the monoclinic phase in GPa. Here, $C_{11}, \ldots, C_{66}$ are the elastic moduli that appear in the standard tetragonal elastic tensor [16]. The tetragonal data is estimated for 1480 K in [2]; see also Table II of [6]. The monoclinic data is given in [2]. To allow for a direct comparison with [6], we take the monoclinic data at 1273 K. No experimental data seems to be available for the orthorhombic phase, which is why we fit the orthorhombic data of [4]. Orthorhombic moduli where no data to be fitted is available are marked by $\star$. Empty entries are zero by symmetry.

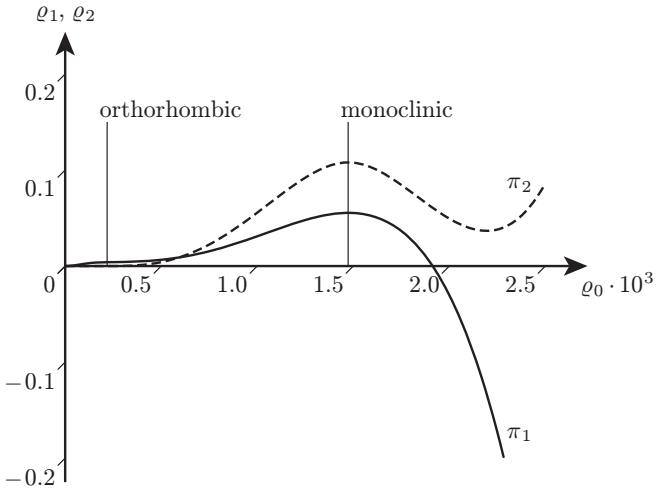

Figure 4: Plots of the path components π_1 (solid line) and π_2 (dashed line) in the Landau construction.

3.2 Two-dimensional Landau energy for zirconia

In the two-dimensional setting in the c_1-c_2-plane of Section 2.3.1, the strain variables are e_1, e_2 and e_6. The position of the three phases with respect to those coordinates is given in Table 1. The invariants (1) then give the location of the phases in the orbit space $\varrho(\mathbb{R}^3)$; see Table 2. Finally, the moduli we want to reproduce are listed in Table 3.

As motivated in Section 3.1, the energy is of the form (4). In particular, the path is parameterized by ϱ_0 and the image of the mapping π has to lie in the half-space $\{(\varrho_1, \varrho_2) \mid \varrho_2 \geq 0\}$. It turns out that π_1 can be defined as a piecewise polynomial function with two quartic segments that join C^2-continuously at the orthorhombic phase. Similarly, π_2 can be constructed by three polynomial pieces (constant, quartic, cubic) with knots at the orthorhombic and the monoclinic phase; see Fig. 4. The profile ϕ_p is defined by two polynomial segments of fifth order and one linear segment that join at the orthorhombic

	range	α_0	α_1	α_2	α_3	α_4	α_5
π_1	$[0, r_1]$	0.0	0.0	$4.7022 \cdot 10^5$	$-2.8200 \cdot 10^9$	$4.8117 \cdot 10^{12}$	
	$[r_1, \infty)$	$2.3135 \cdot 10^{-3}$	$1.9044 \cdot 10^1$	$-8.2030 \cdot 10^4$	$1.5114 \cdot 10^8$	$-5.9481 \cdot 10^{10}$	
π_2	$[0, r_1]$	0.0					
	$[r_1, r_2]$	$-2.5779 \cdot 10^{-3}$	$3.6758 \cdot 10^1$	$-1.8071 \cdot 10^5$	$3.3279 \cdot 10^8$	$-1.3067 \cdot 10^{11}$	
	$[r_2, \infty)$	-2.0020	$3.6905 \cdot 10^3$	$-2.0936 \cdot 10^6$	$3.8059 \cdot 10^8$		
ϕ_p	$[0, r_1]$	0.0	$7.6750 \cdot 10^1$	0.0	$-9.2661 \cdot 10^9$	$5.5386 \cdot 10^{13}$	$-9.3070 \cdot 10^{16}$
	$[r_1, r_3]$	$6.2724 \cdot 10^{-3}$	$-6.9629 \cdot 10^1$	$2.5110 \cdot 10^5$	$-3.2997 \cdot 10^8$	$1.8132 \cdot 10^{11}$	$-3.5698 \cdot 10^{13}$
	$[r_3, \infty)$	$-1.6994 \cdot 10^{-3}$	1.1315				
h_{11}		$9.3250 \cdot 10^1$	$-1.9951 \cdot 10^4$	$1.2759 \cdot 10^7$			
h_{12}		-2.8535					
h_{22}		$7.6778 \cdot 10^1$					
η_0	$[0, r_1]$	$4.7500 \cdot 10^1$	$1.9247 \cdot 10^4$	$-1.7050 \cdot 10^8$	$1.4544 \cdot 10^{11}$	$-3.6269 \cdot 10^{13}$	
	$[r_1, \infty)$	0.0					

Table 4: The coefficients of the parameters for the Landau energy. All functions are polynomials of the form $\sum_j \alpha_j x^j$. For those functions which are defined in a piecewise manner, we list the different polynomial segments and indicate the parameter range over which they are defined. Here, the first two knots are the ϱ_0-coordinates of the orthorhombic and the monoclinic phase, $r_1 := \varrho_0^{\mathrm{o}}$ and $r_2 := \varrho_0^{\mathrm{m}}$ (see Table 2), and the third knot is $r_3 := 1.5557 \cdot 10^{-3}$. All polynomial pieces join C^2-continuously at the knots. The data is rounded to the 4th digit.

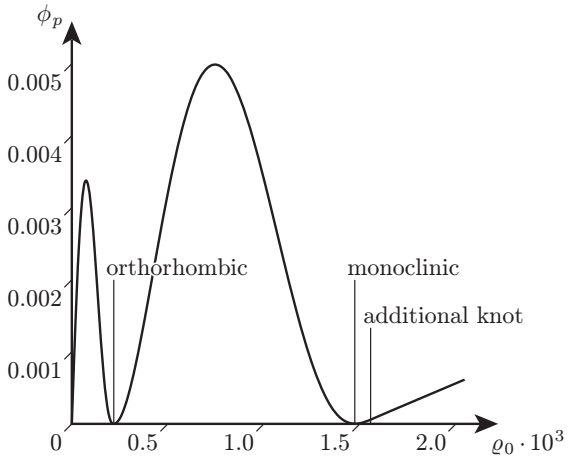

Figure 5: The profile ϕ_p along the path from the tetragonal phase (left, at the origin) via the orthorhombic phase (middle) to the monoclinic phase (right). Since the path is a function of $\varrho_0 = (e_1 - e_2)^2$, only non-negative arguments are meaningful.

phase and a second knot, slightly beyond the monoclinic phase; see Fig. 5. As for the sliding paraboloid $H = (h_{jk})_{j,k=1,2}$, it turns out that it can be modelled by a quadratic function $h_{11}(\varrho_0)$ and constants h_{12}, h_{22}. Finally, the linear contribution η is defined as $\eta(\varrho) := \eta_0(\varrho_0)\varrho_2$, where η_0 is a quartic polynomial between the tetragonal and the monoclinic phase that blends C^2-continuously into the zero function at the monoclinic phase. The energy in (4) with the prescribed degrees of freedom can then be fitted to exactly match the available data; see Table 4 for the parameters.

We call the energy obtained in this way *Landau energy*, since it corresponds to the minimization of all strain parameters other than the order parameters of the full three-dimensional energy.

We remark that in this framework, it is not hard to check that there are no other local minimizers. To do so, it is not necessary to verify that the gradient of the energy vanishes in the interior of the orbit space (though this is possible here since there are no algebraic dependencies of quantities involved).

	range	α_0	α_1	α_2	α_3	α_4	α_5
π_1	$[0, r_1]$	0.0	0.0	$1.8977 \cdot 10^5$	$-6.8075 \cdot 10^8$	$8.9528 \cdot 10^{11}$	
	$[r_1, \infty)$	$8.8152 \cdot 10^7$	$-3.5987 \cdot 10^{10}$				
π_2	$[0, r_1]$	0.0					
	$[r_1, r_2]$	$-2.5754 \cdot 10^{-3}$	$3.6722 \cdot 10^1$	$-1.8053 \cdot 10^5$	$3.3245 \cdot 10^8$	$-1.3050 \cdot 10^{11}$	
	$[r_2, \infty)$	-1.9987	$3.6842 \cdot 10^3$	$-2.0899 \cdot 10^6$	$3.7992 \cdot 10^8$		
ϕ_p	$[0, r_1]$	0.0	$1.3250 \cdot 10^1$	$-1.7613 \cdot 10^5$	$7.7958 \cdot 10^8$	$-1.1488 \cdot 10^{12}$	0.0
	$[r_1, r_3]$	$4.3290 \cdot 10^{-4}$	-4.7852	$1.7116 \cdot 10^4$	$-2.2085 \cdot 10^7$	$1.1849 \cdot 10^{10}$	$-2.2673 \cdot 10^{12}$
	$[r_3, \infty)$	$-3.4429 \cdot 10^{-4}$	$2.2571 \cdot 10^{-1}$				
h_{11}		$1.3250 \cdot 10^1$	$-2.0969 \cdot 10^4$	$1.2759 \cdot 10^7$			
h_{12}		-2.8535					
h_{22}		$7.5620 \cdot 10^1$					
η_0	$[0, r_1]$	$4.7500 \cdot 10^1$	$1.9247 \cdot 10^4$	$-1.7050 \cdot 10^8$	$1.4544 \cdot 10^{11}$	$-3.6269 \cdot 10^{13}$	
	$[r_1, \infty)$	0.0					

Table 5: The coefficients of the parameters for the contribution Φ_{126} to the three-dimensional energy. All functions are polynomials of the form $\sum_j \alpha_j x^j$. For those functions which are defined in a piecewise manner, we list the different polynomial segments and indicate the parameter range over which they are defined. Like in Table 4, the first two knots are $r_1 := \varrho_0^{\mathrm{o}}$ and $r_2 := \varrho_0^{\mathrm{m}}$ (see Table 2), but here the third knot is $r_3 := 1.6182 \cdot 10^{-3}$. All polynomial pieces join C^2-continuously at the knots. The data is rounded to the 4th digit.

a_0	$2.24230 \cdot 10^1$
a_1	$5.86247 \cdot 10^1$
b	$4.56152 \cdot 10^3$
c	$1.05770 \cdot 10^1$

Table 6: The coefficients of the parameters for Φ_{456} defined in (6), which constitutes one contribution to the three-dimensional energy. The data is rounded to the 5th digit.

Instead, we can argue in a simple manner, since the energy function is always decreasing in some direction in the interior of $\varrho(\mathbb{R}^3)$ (except at the global minimizers, which are the t–o–m phases). The same behaviour can be verified for the boundary of the orbit space $\partial\varrho(\mathbb{R}^3)$ by inspecting the restriction of the energy function to the boundary. The coefficients shown in Table 4 have different orders of magnitude since the input data values (the position of phases and the moduli) differ by orders of magnitude; see Tables 2 and 3. Fig. 4 shows that the constructed functions are nevertheless regular, without strong oscillations.

3.3 Three-dimensional energy function for zirconia

The two-dimensional construction can be extended to the full three-dimensional setting in a rather straightforward way. We keep the Landau energy of Section 3.2, here denoted Φ_{126} to indicate its dependence on e_1, e_2 and e_6. Since the energetic contributions to be constructed below contribute to the moduli with indices 1, 2 and 6, the parameters of the Landau construction change, and their new values are given in Table 5.

We augment Φ_{126} additively by a term Φ_{456} in e_4, e_5 and e_6 to fit C_{44}, C_{55} and C_{45}. Here, we work in strain space, rather than in orbit space, and employ the invariants ϱ_2 and

$$\begin{aligned} \varrho_8(e_1, \ldots, e_6) &:= e_1^2 e_4^2 + e_2^2 e_5^2, \\ \varrho_9(e_1, \ldots, e_6) &:= (e_4^2 + e_5^2)(1 + e_6^2) + 4 e_4 e_5 e_6. \end{aligned} \tag{5}$$

It is easy to verify that $\varrho_8 = \varrho_1\varrho_7 + \frac{1}{4}(\varrho_0 - \varrho_1^2)\varrho_4$ and $\varrho_9 = (1 + \varrho_2)\varrho_4 + 4\varrho_6$. The two latter invariants

	range	α_0	α_1	α_2	α_3	α_4	α_5	α_6
π_1	$[0, r_1]$	0.0	$3.048 \cdot 10^2$	$-1.459 \cdot 10^6$	$2.324 \cdot 10^9$			
	$[r_1, \infty)$	$2.460 \cdot 10^{-2}$	$-3.294 \cdot 10^1$	$8.656 \cdot 10^4$	$-3.411 \cdot 10^7$			
π_2	$[0, r_1]$	0.0						
	$[r_1, r_4]$	$-7.825 \cdot 10^{-3}$	$1.172 \cdot 10^2$	$-6.299 \cdot 10^5$	$1.421 \cdot 10^9$	$-1.206 \cdot 10^{12}$	$4.376 \cdot 10^{14}$	$-5.784 \cdot 10^{16}$
	$[r_4, \infty)$	$8.494 \cdot 10^{-2}$						
π_3	$[0, r_1]$	0.0	$2.285 \cdot 10^2$	$-1.012 \cdot 10^6$	$1.492 \cdot 10^9$			
	$[r_1, \infty)$	$1.538 \cdot 10^{-2}$	$1.732 \cdot 10^1$	$-4.550 \cdot 10^4$	$1.793 \cdot 10^7$			
ϕ_p	$[0, r_1]$	0.0	$6.350 \cdot 10^1$	0.0	$-7.647 \cdot 10^9$	$4.565 \cdot 10^{13}$	$-7.660 \cdot 10^{16}$	
	$[r_1, r_3]$	$5.511 \cdot 10^{-3}$	$-6.118 \cdot 10^1$	$2.207 \cdot 10^5$	$-2.902 \cdot 10^8$	$1.596 \cdot 10^{11}$	$-3.145 \cdot 10^{13}$	
	$[r_3, \infty)$	$-1.427 \cdot 10^{-3}$	$9.504 \cdot 10^{-1}$					
h_{11}		$8.000 \cdot 10^1$	$1.018 \cdot 10^3$					
h_{13}		-7.153						
h_{22}		1.158						
h_{33}		$8.250 \cdot 10^1$	$4.412 \cdot 10^3$					

Table 7: The coefficients of the parameters for the contribution Φ_3 to the three-dimensional energy. All functions are polynomials of the form $\sum_j \alpha_j x^j$. For those functions which are defined in a piecewise manner, we list the different polynomial segments and indicate the parameter range over which they are defined. The knots are $r_1 := \varrho_0^{\mathrm{o}}$, $r_2 := \varrho_0^{\mathrm{m}}$ (see Table 2), $r_3 := 1.554 \cdot 10^{-3}$ and $r_4 := 2.210 \cdot 10^{-3}$. All polynomial pieces join C^2-continuously at the knots. The data is rounded to the 3rd digit.

are chosen since they are non-negative. It turns out that the ansatz

$$\Phi_{456} := (a_0 + a_1\varrho_2)\varrho_4 + b\varrho_8 + c\varrho_9 \tag{6}$$

is sufficient to fit the moduli C_{44}, C_{45} and C_{55}. This form is considerably simpler than the contributions defined in orbit space, but possible only because so few moduli need to be fitted. Since Φ_{456} is non-negative, it is easy to verify that minima exist only at the tetragonal, the orthorhombic and the monoclinic phase. The parameters for Φ_{456} are given in Table 6.

To match the elastic moduli involving the strain component e_3, we employ the path-profile construction with the four invariants $\tilde{\varrho}_0 := \varrho_0$, $\tilde{\varrho}_1 := \varrho_1 + \varrho_3$, $\tilde{\varrho}_2 := \varrho_2$, $\tilde{\varrho}_3 := \varrho_3$. Again, we choose the invariant $\tilde{\varrho}_0$ for the parameterization of the path, the profile and the sliding paraboloid. As for the latter, it turns out that it suffices to involve only h_{11}, h_{13} , h_{22} and h_{33}, and set the other components to zero. Moreover, the linear contribution η is not needed for this energetic contribution that we denote Φ_3; see Table 7 for details.

An energy that fits exactly all available moduli is then

$$\Phi := \Phi_{126} + \Phi_{456} + \Phi_3, \tag{7}$$

considered as a function in strain space, that is, the invariants are evaluated with the strain variables.

An examination of the energy reveals that no global minimizers other than the prescribed ones exist. Local minimizers could in principle exist due to the addition of three energetic terms, because gradients could cancel out locally. An analysis of the saddle point via Newton search as in [11] could be employed to examine the existence of local minima.

4 Discussion

For theory and applications of solid phase transitions alike, it is of general interest to have a methodology which allows to fit experimental data for multi-phase materials in a simple and phenomenological, yet natural way. We here propose the *path-profile construction*. The intuition behind this method is the observation that a good phenomenological description of the energy landscape needs to describe the local properties of the stable phases correctly, and has to offer a phenomenologically appropriate transformation path. The classical approach with invariant polynomials is well suited for the former,

but not for the latter. We develop a method to model a phenomenological transformation path such that local properties can be fitted with relative ease. The approach has recently been used in a less explicit fashion to model one contribution to an energy for InTl [11]. Here, we demonstrate the simplicity of the method by choosing a material with a triple point. We first derive the Landau contribution, which only relies on order parameters, and apply the path-profile construction. The energy as a function of the three-dimensional strain tensor is then obtained via extension.

The approach proposed here is general, even if the specific examples are genuine for zirconia. We noticed that the process of fitting is remarkably easy as the construction with the sliding paraboloid facilitates the process greatly. The calculations for the fitting process were done in Maple, where a straightforward implementation requires a few seconds to execute on a personal computer.

It is possible to construct the energy entirely in orbit space rather than composing it of three different terms as done here. Though the approach to work in the full orbit space may be more elegant and ultimately more straightforward, there remain some technical aspects to overcome. Namely, it becomes more difficult to rule out minima on the boundary. This will be investigated in future work. Also, it is not immediate which set of invariants should be chosen. In the low-dimensional approach advocated here, it is easy to test and compare different choices, while the analogous procedure becomes much more involved when the number of invariants involved is increased.

It has been noted that using a lowest-order polynomial as the Gibbs energy density necessarily introduces a second orthorhombic phase for which experimental evidence seems to be unavailable [6]. While this phase is stable at zero pressure only for a small range of temperatures above 1520 K and becomes unstable for pressure over 1.35 GPa [6], it has been shown to be the most stable phase for the polynomial energy under various shear loads at room conditions [7]. Since the existence of this phase may have implications on zirconia as a toughening agent near crack tips, it seems desirable to examine whether other energy densities also predict this phase. The present isothermal energy density may serve as a basis for such investigations.

Acknowledgements

The Interactive Ideas Factory at the University of Bath, an EPSRC Bridging the Gaps project (EP/E018122/1) funded a visit of J. Z. to Clausthal University of Technology, during which most of the work reported here was carried out. J. Z. gratefully acknowledges the financial support of the EPSRC through an Advanced Research Fellowship (GR/S99037/1). We thank Kaushik Dayal and Heinrich-Gregor Zirnstein for helpful comments.

References

[1] S.-K. Chan. The polymorphic transformations of zirconia. *Physica B+C*, 150(1–2):212–222, May 1988.

[2] S.-K. Chan, Y. Fang, M. Grimsditch, Z. Li, M. V. Nevitt, W. M. Robertson, and E. S. Zouboulis. Temperature-dependence of the elastic moduli of monoclinic zirconia. *Journal of the American Ceramic Society*, 74(7):1742–1744, July 1991.

[3] C. Chevalley. Invariants of finite groups generated by reflections. *American Journal of Mathematics*, 77(4):778–782, Oct. 1955.

[4] P. W. Dondl and J. Zimmer. Modeling and simulation of martensitic phase transitions with a triple point. *Journal of the Mechanics and Physics of Solids*, 52(9):2057–2077, Sept. 2004.

[5] J. L. Ericksen. Some phase transitions in crystals. *Archive for Rational Mechanics and Analysis*, 73(2):99–124, June 1980.

[6] G. Fadda, L. Truskinovsky, and G. Zanzotto. Unified Landau description of the tetragonal, orthorhombic, and monoclinic phases of zirconia. *Physical Review B*, 66(17):174107, Nov. 2002.

[7] G. Fadda, L. Truskinovsky, and G. Zanzotto. Nonhydrostatic stabilization of an orthorhombic phase of zirconia. *Physical Review B*, 68(13):134106, Oct. 2003.

[8] F. Falk and P. Konopka. Three-dimensional Landau theory describing the martensitic phase transformation of shape-memory alloys. *Journal of Physics: Condensed Matter*, 2(1):61–77, Jan. 1990.

[9] R. J. Gooding, Y. Y. Ye, C. T. Chan, K.-M. Ho, and B. N. Harmon. Role of non-symmetry-breaking order parameters in determining the martensitic energy barrier: The bcc-to-9R transformation. *Physical Review B*, 43(16):13626–13629, June 1991.

[10] G.-M. Greuel, G. Pfister, and H. Schönemann. SINGULAR 2.0. A computer algebra system for polynomial computations, Centre for Computer Algebra, University of Kaiserslautern, 2001. `http://www.singular.uni-kl.de`.

[11] K. Hormann and J. Zimmer. On Landau theory and symmetric energy landscapes for phase transitions. *Journal of the Mechanics and Physics of Solids*, 55(7):1385–1409, July 2007.

[12] Y. Huo and I. Müller. Interfacial and inhomogeneity penalties in phase transitions. *Continuum Mechanics and Thermodynamics*, 15(4):395–407, Aug. 2003.

[13] R. D. James. Unpublished notes. Private communication, 1988.

[14] A. Kuwabara, T. Tohei, T. Yamamoto, and I. Tanaka. *Ab initio* lattice dynamics and phase transformations of ZrO_2. *Physical Review B*, 71(6):064301, Feb. 2005.

[15] L. D. Landau. On the theory of phase transitions. In D. ter Haar, editor, *Collected papers of L. D. Landau*. Gordon & Breach, New York, 1965.

[16] A. E. H. Love. *A Treatise on the Mathematical Theory of Elasticity*. Dover, New York, fourth edition, 1944.

[17] N. Simha and L. Truskinovsky. Shear induced transformation toughening in ceramics. *Acta Metallurgica et Materialia*, 42(11):3827–3836, Nov. 1994.

[18] G. F. Smith and R. S. Rivlin. The strain-energy function for anisotropic elastic materials. *Transactions of the American Mathematical Society*, 88(1):175–193, May 1958.

[19] L. Truskinovsky and G. Zanzotto. Elastic crystals with a triple point. *Journal of the Mechanics and Physics of Solids*, 50(2):189–215, Feb. 2002.

[20] H. Weyl. *The Classical Groups: Their Invariants and Representations*. Princeton Landmarks in Mathematics and Physics. Princeton University Press, Princeton, NJ, second edition, 1997. Fifteenth printing.

[21] J. Zimmer. Stored energy functions for phase transitions in crystals. *Archive for Rational Mechanics and Analysis*, 172(2):191–212, May 2004.